0026-895X/07/7106-1535–1544$20.00
MOLECULAR PHARMACOLOGY
Copyright © 2007 The American Society for Pharmacology and Experimental Therapeutics
Mol Pharmacol 71:1535–1544, 2007

Vol. 71, No. 6
34371/3204321
Printed in U.S.A.

Mechanism of Thiazolidinedione-Dependent Cell Death in Jurkat T Cells

Mathias Soller, Stefan Dröse, Ulrich Brandt, Bernhard Brüne, and Andreas von Knethen

Department of Biochemistry I, Pathobiochemistry (M.S., B.B., A.v.K.) and Molecular Bioenergetics (S.D., U.B.), Johann Wolfgang Goethe University Frankfurt, Faculty of Medicine, Frankfurt am Main, Germany

Received January 23, 2007; accepted February 26, 2007

ABSTRACT

Thiazolidinediones are synthetic agonists for the transcription factor peroxisome proliferator-activated receptor γ (PPARγ) and are therapeutically used as insulin sensitizers. Besides therapeutical benefits, potential side effects such as the induction of cell death by thiazolidinediones deserve consideration. Although PPARγ-dependent and -independent cell death in response to thiazolidinediones has been described, we provide evidence supporting a new mechanism to account for thiazolidinedione-initiated but PPARγ-independent cell demise. In Jurkat T cells, ciglitazone and troglitazone provoked rapid and dose-dependent cell death, whereas rosiglitazone did not alter cell viability. We found induction of apoptosis by troglitazone, whereas ciglitazone caused necrosis. Because preincubation with the reactive oxygen species (ROS) scavengers manganese (III) tetrakis(4-benzoic acid) porphyrin and vitamin C significantly inhibited ciglitazone- and partially troglitazone-mediated cell death, we suggest that ROS contribute to cytotoxicity. Assuming that ROS originate from mitochondria, studies in submitochondrial particles demonstrated that all thiazolidinediones inhibited complex I of the mitochondrial respiratory chain. However, only ciglitazone and troglitazone lowered complex II activity as well. Pharmacological inhibition of complexes I and II documented that complex II inhibition in Jurkat cells caused massive apoptotic cell death, whereas inhibition of complex I provoked only marginally apoptosis after 4-h treatment. Therefore, inhibition of complex II by ciglitazone and troglitazone is the main trigger of cell death. ATP depletion by ciglitazone, in contrast to troglitazone, is responsible for induction of necrosis. Our results demonstrate that despite their similar molecular structure, thiazolidinediones differently affect cell death, which might help to explain some adverse effects occurring during thiazolidinedione-based therapies.

The transcription factor peroxisome proliferator-activated receptor γ (PPARγ) is a member of the nuclear hormone receptor superfamily. Three isoforms, PPARα, PPARβ/δ, and PPARγ, have been identified so far. Among these, PPARγ is best characterized because of its therapeutic potential for treatment of diabetes type 2. However, PPARγ is also known for its involvement in several other human pathological settings, including atherosclerosis, cancer, and inflammation (Kersten et al., 2000). DNA binding by PPARγ as a transcription factor requires heterodimerization with the 9-*cis*-retinoic acid receptor and binding of an agonist. Natural agonists of PPARγ originate from the metabolism of arachidonic acid, including leukotrienes, hydroxyeicosatetraenoic acids, and prostaglandins (Daynes and Jones, 2002). Thiazolidinediones (TZDs) such as ciglitazone, troglitazone, and rosiglitazone represent a group of synthetic PPARγ agonists. Most synthetic agonists belong to the class of above-mentioned TZDs, but non-TZD synthetic agonists have been described previously (Rybczynski et al., 2003). Activated PPARγ, especially in T cells, is involved in the regulation of immune responses and cell survival signaling (Harris and Phipps, 2000, 2001, 2002; Tautenhahn et al., 2003; Soller et al., 2006). This finding is important in patients with type 2 diabetes who are medicated by TZDs as known insulin-sensitizers. Therefore, activation of PPARγ in these pa-

This work was supported by grants from Deutsche Forschungsgemeinschaft (BR999), Krebshilfe, and Sander Foundation.
Article, publication date, and citation information can be found at http://molpharm.aspetjournals.org.
doi:10.1124/mol.107.034371.

ABBREVIATIONS: PPARγ, peroxisome proliferator-activated receptor γ; ROS, reactive oxygen species; 2-DG, 2-deoxy-D-glucose; CIG, ciglitazone; DAPI, 4′,6-diamidino-2-phenylindol; DBQ, *n*-decylubiquinone; DCIP, dichlorphenolindophenol; DiOC6(3), 3.3-dihexyloxacarbocyanide iodide; H_2DCF-DA, 2′,7′-dichlorodihydrofluorescein diacetate; MnTBAP, manganese (III) tetrakis(4-benzoic acid) porphyrin; NAC, *N*-acetylcysteine; PI, propidium iodide; ROSI, rosiglitazone; Rot, rotenone; SMP, submitochondrial particle; STS, staurosporine; TRO, troglitazone; TTFA, 2-thenoyltrifluoroacetone; TZD, thiazolidinedione; $\Delta\Psi_M$, mitochondrial membrane potential; RT, reverse transcriptase; PCR, polymerase chain reaction; RT-PCR, reverse-transcriptase polymerase chain reaction; GAPDH, glyceraldehyde 3-phosphate dehydrogenase; FITC, fluorescein isothiocyanate; PBS, phosphate-buffered saline; DMSO, dimethyl sulfoxide; TPA, 12-*O*-tetradecanoylphorbol-13-acetate; WY14643, pirinixic acid.

tients might provoke an inhibited immune response by the induction of cell death.

However, actions of TZDs are currently discussed because of the increasing number of publications describing their effects by activating pathways independently from PPARγ signaling. The argument that TZDs can exert receptor-independent effects is based on observations that concentrations needed to observe TZD actions were much higher than their EC_{50} values, PPARγ antagonists failed to inhibit TZD-evoked responses, and effects occurred rapidly and often without PPARγ expression (Feinstein et al., 2005). Therefore, we focused our interest in the present study on PPARγ-independent effects of the TZDs ciglitazone, troglitazone, and rosiglitazone in Jurkat T cells. Among these mentioned TZDs, rosiglitazone is currently used as an antidiabetic drug, whereas the therapeutic use of troglitazone was stopped because of its liver intoxication (Tolman, 2000).

Recent studies dealing with PPARγ-independent effects of TZDs point at mitochondria as primary targets. In this respect, a rapid decrease in mitochondrial membrane potential ($\Delta\Psi_M$) seems to be one major event, especially after troglitazone and ciglitazone treatment. Troglitazone quickly induced mitochondrial dysfunction and increased permeability, calcium influx, nuclear condensation, and caspase-3 activation in HepG2 hepatocarcinoma cells (Haskins et al., 2001; Bova et al., 2005). Rapid effects were observed in response to ciglitazone, which also induced break-down of $\Delta\Psi_M$, increased ROS production in astrocytes, and enhanced lactate production in leukemia (HL-60) cells (Pérez-Ortiz et al., 2004; Scatena et al., 2004). These data suggest that TZDs affect mitochondrial respiration, causing changes in the glycolytic metabolism. Indeed, it has been shown that complex I is inhibited by TZDs (Brunmair et al., 2004; Scatena et al., 2004), supporting the hypothesis that several effects attributed to TZDs are caused by their impact on mitochondria. Taking into consideration that TZDs are discussed as therapeutics for the treatment of cancer and various inflammatory and neurodegenerative diseases (Pershadsingh, 2004), beside their current use for the treatment of diabetes type 2, a better understanding of TZD signaling in various tissues is essential for future drug design.

Materials and Methods

Materials. Ciglitazone, troglitazone, rosiglitazone, staurosporine, and manganese (III) tetrakis(4-benzoic acid) porphyrin (MnTBAP) were obtained from Alexis (Grünberg, Germany). H_2DCF-DA was obtained from Invitrogen (Leiden, The Netherlands). All other chemicals were purchased from Sigma (Taufkirchen, Germany) or Carl Roth GmbH and Co. (Karlsruhe, Germany) in analytical quality.

Cell Culture. We cultivated Jurkat cells in 24-well plates (Falcon; BD Biosciences Discovery Labware, Heidelberg, Germany) using RPMI 1640 medium supplemented with 100 U/ml penicillin, 100 μg/ml streptomycin, and 10% heat-inactivated fetal calf serum (all from Biochrom, Berlin, Germany).

mRNA Analysis. We extracted RNA from Jurkat cells using peqGOLD RNAPure (Peqlab, Erlangen, Germany) according to the distributor's manual. For the reverse transcriptase (RT) reactions, we used the Advantage RT-for-PCR kit (Clontech/Takara Bio Europe, Saint-Germain-en-Laye, France). PCR for human PPARγ and glyceraldehyde 3-phosphate dehydrogenase (GAPDH) was performed using the MasterTaq-Kit (Eppendorf, Hamburg, Germany). Sequences of the primers were as follows: PPARγ (accession number NM138712; 613-1324), T_A = 62°C: 5′-CAT GCT TGT GAA GGA TGC AAG GG-3′, T_A = 62°C 3′-GGA CGC TTT CGG AAA ACC ACT GA-5′; GAPDH (accession number NM002046; 76-1083), T_A = 63°C 5′-ATGGGGAAGGTGAAGGTCGGAGT-3′; T_A = 63°C 3′-GGGTG-TACCGGAGGTTCCTCATT-5′. Products were run on a 1% agarose gel followed by ethidium bromide staining. We calculated annealing temperatures using the primer design program Oligo (Molecular Biology Insights, Cascade, CO). Controls of isolated RNA omitting RT during PCR were used to guarantee genomic DNA-free RNA preparations (data not shown).

Measurement of $\Delta\Psi_M$. After individual incubations, cells were loaded with 40 nM fluorochrome 3.3-dihexyloxacarbocyanide iodide [$DiOC_6$(3); Invitrogen] for 15 min, after which the dye is accumulated in mitochondria containing an intact membrane potential. After indicated treatments, $\Delta\Psi_M$ was measured by a FACSCanto flow cytometer using FACSDiva software (both from BD Biosciences, Heidelberg, Germany). At least 10,000 cells were accumulated for analysis. Results are expressed as the percentage of total cells with $\Delta\Psi_M$ breakdown (dead cells).

Annexin V-FITC/PI Staining. To determine the amount of apoptotic and necrotic cells, we used an annexin V-FITC/PI staining kit (Immunotech, Krefeld, Germany). Detection was performed as described in the distributor's manual. After incubations, 2×10^5 cells were labeled with 1 μl of annexin V-FITC and 2.5 μl of PI in 100 μl of binding buffer for 15 min on ice in the dark. Afterward, 150 μl of binding buffer was added, and cell samples were analyzed immediately using a FACSCanto flow cytometer and FACSDiva software. Apoptosis was assessed when cells were annexin V-FITC single-positive. Annexin V-FITC/PI double-positive cells were considered as secondary necrotic or necrotic. A minimum of 10,000 cells was analyzed.

DAPI Staining. Jurkat cells (5×10^5) were treated as indicated. Thereafter, cells were washed with PBS and fixed in 4% paraformaldehyde for 25 min followed by a 5-min washing step in PBS. Afterward, cells were permeabilized using 0.2% Triton X-100 and washed two times again with PBS. Finally, cells were stained with DAPI (6×10^{-7} M) for 10 min. Detection was done by fluorescence microscopy (Zeiss, Goettingen, Germany) using AxioVision Software (Carl Zeiss MicroImaging GmbH, Goettingen, Germany).

Cytochrome *c* Release Assay. Mitochondrial cytochrome *c* release was determined by Western blot analysis of cytosolic cytochrome *c*, as described elsewhere (Leist et al., 1998). In brief, cells (4×10^6) were harvested by centrifugation and resuspended in 250 μl of PBS at room temperature. Next, 250 μl of a digitonin/sucrose solution (40 μg of digitonin in 500 mM sucrose/4×10^6 cells) was added for 30 s, and the samples were subsequently centrifuged at 10,000*g* for 1 min. Cytosolic supernatants (30 μg) were subjected to SDS-polyacrylamide gel electrophoresis (15% gels), and Western blot analysis using an anti-cytochrome *c* antibody (BD PharMingen, Hamburg, Germany) was performed.

Determination of ROS Production. For the detection of intracellular-produced oxidants, Jurkat cells were preloaded with 10 μM H_2DCF-DA (Invitrogen) for 1 h at 37°C. Cells were then pelleted and washed two times with PBS. Afterward, cells were incubated with indicated treatments for 2 h followed by two washing steps with PBS. Fluorescence was measured in 10,000 cells/sample by flow cytometry (FACSCanto) with excitation and emission settings of 488 and 525 nm, respectively.

Isolation of Bovine Heart Submitochondrial Particles. Submitochondrial particles (SMPs) were prepared from bovine heart mitochondria as described by Okun et al. (1999b) but were eventually diluted in SMP buffer containing 75 mM sodium phosphate/1 mM $MgCl_2$/1 mM sodium-EDTA, pH 7.4. The protein concentration determined by the Lowry method (Lowry et al., 1951) was 67 mg/ml, the cytochrome *b* concentration was 34.8 μM, and the cytochrome a/a_3 concentration was 39.2 μM.

Determination of Complex I Activities. NADH-oxidase (complex I) activity was determined in measurements with the Oxygraph-2K (Oroboros, Innsbruck, Austria). For that, SMPs (33.5 μg of

protein) were added to 2 ml of SMP buffer at 25°C with 0.5 mM NADH as substrate for complex I. Oxygen consumption was measured for 15 min after the indicated treatments at 25°C and calculated as a percentage of untreated controls (set as 100%). For the determination of NADH:ubiquinone oxidoreductase activity of SMPs (23.5 μg of protein per assay), 100 μM *n*-decylubiquinone (DBQ; dissolved in DMSO) and 100 μM NADH were used as substrates. NADH oxidation ($\varepsilon_{340-400\ nm}$ = 6.1 $mM^{-1}cm^{-1}$) rates were recorded in the presence of 2 mM KCN at 30°C using a Shimadzu Multi Spec-1501 diode array spectrophotometer.

Determination of Complex II Activities. To determine succinate-oxidase activity, SMPs (67 μg of protein) were added to 2 ml of SMP buffer containing 5 mM sodium succinate as substrate for complex II. Oxygen consumption was measured at 25°C using an Oxygraph-2K system, and TZDs were added cumulatively to the maximal concentrations indicated in the figure legend. For direct determination of complex II activity, SMPs (67 μg of protein) were incubated in SMP buffer containing 5 mM sodium succinate as substrate and inhibitors for complex I (1.5 μM rotenone), complex III (3 μM antimycin A), and complex IV (2 mM KCN) for 10 min at 25°C. Then, 2% dichlorphenolindophenol (DCIP) was added, followed by indicated treatments. Succinate dehydrogenase (complex II) catalyzes the reaction from succinate to fumarate involving electron transfer to ubiquinone. Reduced ubiquinone was reoxidized by DCIP, which could be detected as reduced DCIP at 610 nm (with 750 nm as reference) using a Shimadzu Multi Spec-1501 diode array spectrophotometer.

ATP Measurement. For ATP determination, a commercially available luciferin-luciferase assay kit (ATP Bioluminescent Assay Kit; Sigma) was used. In brief, 5×10^5 Jurkat cells were treated as indicated for 2 h and lysed with 100 μl of lysing buffer. ATP determination was performed according to the distributor's manual. Whole-cell ATP content was detected by running an internal standard. The cellular ATP level was converted to the percentage of untreated cells (control was set as 100%).

Statistical Analysis. We used two-tailed statistical analysis to evaluate the data. Results are expressed as the mean ± S.D. or ± S.E. Experiments were evaluated using the Student's *t* test. We considered *P* values ≤ 0.05 (∗) as significant.

Results

Selection of a PPARγ Negative Jurkat Subclone. To analyze TZD effects in T cells independent from PPARγ, we analyzed in a first set of experiments a panel of Jurkat clones from our own and other laboratories for PPARγ expression. As shown in Fig. 1A, second lane, and Fig. 1B, first lane, one subclone did not express PPARγ in resting conditions, whereas others were PPARγ-positive (data not shown), which is in line with previous data (Tautenhahn et al., 2003). To test whether TZD treatment will express PPARγ in this Jurkat subclone, we stimulated cells with 30 μM ciglitazone for 4 h. RT-PCR revealed no PPARγ expression after ciglitazone treatment (Fig. 1A, third lane). However, this subclone is able to express PPARγ mRNA after T-cell activation by TPA stimulation for 15 h as shown in Fig. 1B, second lane. But because this Jurkat subclone showed no PPARγ expression in conditions used in this study, it was referred to as Jurkat P^- and represents a suitable test system to study PPARγ-independent effects of TZDs.

TZDs Affect $\Delta\Psi_M$. After treatment with TZDs, we analyzed the $\Delta\Psi_M$ by $DiOC_6(3)$ as a first marker of cell death in Jurkat P^- cells. $DiOC_6(3)$-negative cells have lost their $\Delta\Psi_M$ and are defined as dead cells. A 4-h treatment of Jurkat P^- cells with increasing concentrations (30–100 μM) of ciglitazone and troglitazone provoked a fast decrease of $\Delta\Psi_M$. The highest concentration of ciglitazone (100 μM) caused 55% cell death (Fig. 2, ●), whereas the same concentration of troglitazone induced cell death in approximately 40% of cells (Fig. 2, ○). Thus, ciglitazone is more effective than troglitazone in causing cell death in Jurkat P^- T cells. However, rosiglitazone showed no depolarization of $\Delta\Psi_M$ and consequently did not alter cell viability at any concentration up to 100 μM (Fig. 2, ▲).

TZDs Initiate Different Modes of Cell Death. In contrast to rosiglitazone, ciglitazone and troglitazone led to a loss of $\Delta\Psi_M$, which represents an early event after cell death induction. To clearly define the type of cell death induced by ciglitazone and troglitazone, we performed an annexin V-

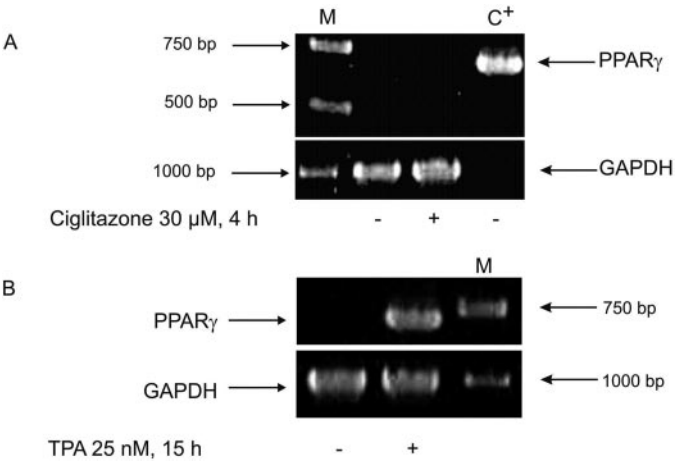

Fig. 1. PPARγ mRNA expression in Jurkat cells. Jurkat cells were treated with 30 μM ciglitazone for 4 h (A) or with 25 nM TPA for 15 h (B) or remained as controls, followed by RT-PCR analysis for PPARγ and GAPDH as described under *Materials and Methods.* A, agarose gel electrophoresis shows PCR products for PPARγ and GAPDH from untreated (second lane) and ciglitazone treated (third lane) Jurkat cells and a 1-kilobase DNA ladder (M) in the first lane. The fourth lane (C^+) shows the PCR product obtained from a plasmid containing full PPARγ. B, PPARγ and GAPDH PCR products from untreated cells (first lane) and TPA-treated cells (second lane), and a 1-kb DNA ladder (third lane) is shown. Data are representative of three separate RT-PCR analyses.

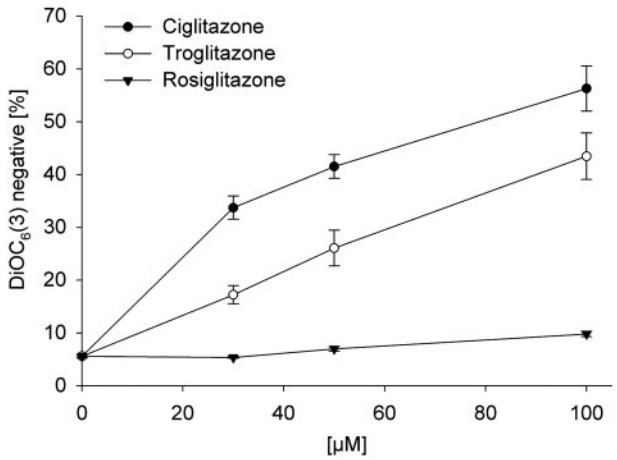

Fig. 2. TZD-induced cell death in Jurkat P^- cells. Jurkat P^- cells were treated with increasing concentrations of ciglitazone, troglitazone, and rosiglitazone from 30 to 100 μM for 4 h. Survival of cells was analyzed by flow cytometry using $DiOC_6(3)$ as described under *Materials and Methods.* Cell death is expressed as a percentage of $DiOC_6(3)$-negative cells of whole-cell population. Values are means ± S.E., n = 12.

FITC/PI assay 4 h after treatment. As expected, incubation of Jurkat P$^-$ cells with rosiglitazone (Fig. 3A; ROSI) showed no significant induction of apoptosis compared with control (Fig. 3A, ROSI, 2.8%, versus control, 1.9%), whereas troglitazone (Fig. 3A, TRO) caused predominantly apoptosis, thus showing 17.1% annexin V-FITC single-positive cells and a minor fraction of double-positive (i.e., necrotic cells). In contrast, in cells incubated for 4 h with ciglitazone, we detected 27.8% annexin V-FITC/PI double-positive cells (Fig. 3A, CIG) without any significant increase in annexin V-FITC single-positive (Fig. 3A CIG 5.3% versus 1.9% of control) and thus apoptotic cells compared with the control. This finding implies a necrotic type of cell death after ciglitazone addition. The functionality of the annexin V-FITC/PI staining protocol was assured, using the classic apoptotic trigger staurosporine (Fig. 3A, STS), which showed typical apoptotic characteristics represented by annexin V-FITC single-positive cells (75.1%) and a smaller portion (17.2%) of annexin V-FITC/PI double-positive and thus secondary necrotic cells. Similar results in discriminating between necrosis and apoptosis induced by ciglitazone and troglitazone were obtained by DAPI staining (Fig. 3B). Nuclei from troglitazone-treated cells (Fig. 3B, TRO) and STS-treated cells (Fig. 3B, STS) showed condensed chromatin, a hallmark of apoptosis. Arrows in Fig. 3B mark apoptotic nuclei with condensed chromatin. In line with the annexin V-FITC/PI assay, nuclei of ciglitazone-treated cells (Fig. 3B, CIG) and rosiglitazone-treated cells (Fig. 3B, ROSI) did not reveal apoptotic criteria. Thus, data obtained from DAPI staining further support the assumption that troglitazone induces apoptosis, whereas ciglitazone provokes necrosis as the underlying mechanism of cell death in Jurkat P$^-$ T cells.

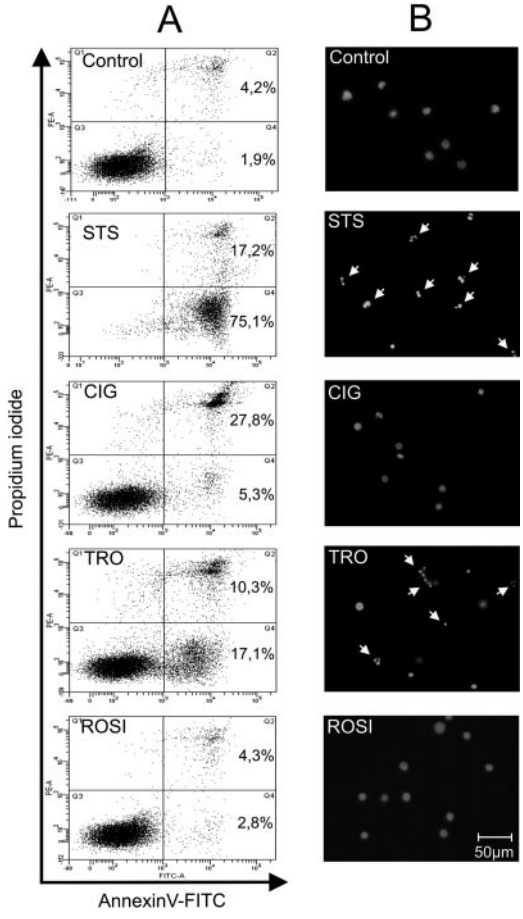

Fig. 3. Characterization of cell death induction by ciglitazone and troglitazone. Jurkat P$^-$ cells were treated with 0.5 μg/ml staurosporine (STS) as an established inducer of apoptosis, 50 μM ciglitazone (CIG), 100 μM troglitazone (TRO), and 100 μM rosiglitazone (ROSI) or left untreated (Control) for 4 h. A, cells were collected and washed, followed by annexin V-FITC/PI staining to distinguish apoptosis versus necrosis using flow cytometry as described under *Materials and Methods.* Data are representatives of three separate experiments. B, representative images of DAPI-stained untreated, STS, CIG, TRO, and ROSI incubated Jurkat P$^-$ cells detected by fluorescence microscopy as described under *Materials and Methods.* Arrows mark cells with condensed chromatin. Magnification, 400×.

In Contrast to Troglitazone, Ciglitazone Does Not Induce Cytochrome *c* Release. To confirm necrosis for ciglitazone-induced cell death and apoptosis for troglitazone-induced cell death as the underlying mechanism, we analyzed cytochrome *c* release from the mitochondria to the cytosol. This is considered an early event during the apoptotic process, which should not occur during necrosis. Therefore, we analyzed cytochrome *c* release at 2 and 4 h after 50 μM troglitazone (Fig. 4A) and 50 μM ciglitazone (Fig. 4B) treatment. We could not detect translocation of cytochrome *c* at indicated time points after ciglitazone addition (Fig. 4B, lanes 2 and 3), whereas troglitazone treatment led to release of cytochrome *c* to the cytosol starting at 2 h after treatment (Fig. 4A, lanes 3 and 4) confirming induction of apoptosis as already detected by annexin V-FITC/PI staining. STS was used as a positive control, which induced the release of cytochrome *c* to the cytosol after a 4-h treatment (Fig. 4A, lane 4). Furthermore, we could show that the inhibition of complexes I and II of respiratory chain by the combination of rotenone/TTFA also leads to cytochrome *c* release after 4-h treatment (Fig. 4B, lane 1) and therefore induces apoptosis.

TZDs Significantly Induce ROS Production in Jurkat P$^-$ Cells. The generation of ROS is a general mechanism contributing to induction of necrosis (Jäättelä and Tschopp, 2003) and apoptosis. TZDs are known to induce ROS production in Jurkat cells (Atarod and Kehrer, 2004). Based on our

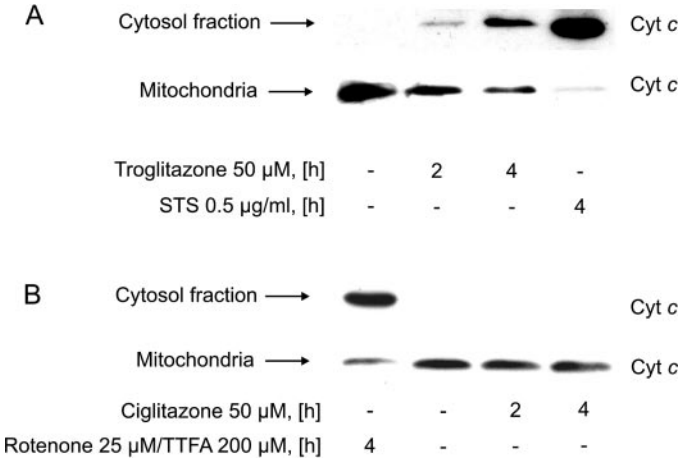

Fig. 4. Troglitazone induces cytochrome *c* release, whereas ciglitazone-mediated cell death is unrelated to cytochrome *c* release. Jurkat P$^-$ cells were incubated with 50 μM troglitazone and staurosporine 0.5 μg/ml (STS) as a classic inducer of apoptosis (A) or with 50 μM ciglitazone and the combination rotenone (inhibitor of complex I) 25 μM/TTFA (inhibitor of complex II) 200 μM for times indicated (B) or remained as controls. Cytosolic cytochrome *c* versus mitochondrial cytochrome *c* were determined by immunoblot analysis as described under *Materials and Methods.* One representative blot of three is shown.

finding that TZDs induce different modes of cell death, we compared relative ROS production provoked by ciglitazone, troglitazone, and rosiglitazone (Fig. 5). All tested TZDs significantly induced ROS production compared with DMSO-treated control. Among the tested TZDs, troglitazone was the strongest inductor of ROS production (Fig. 5, column 3), whereas ciglitazone and rosiglitazone produced equal amounts of ROS (Fig. 5, columns 2 and 4). Because disruption of respiratory chain is known as an important inductor of ROS production by mitochondria (Pelicano et al., 2003), inhibition of complexes I and II by their specific inhibitors rotenone and TTFA served as the positive control, which led to strong ROS production (Fig. 5, column 5).

Ciglitazone-Mediated Necrosis Is ROS- and Hydrogen Peroxide-Dependent, whereas Troglitazone-Induced Apoptosis Is Only Partially Mediated by ROS Production. To investigate the role of TZD-induced ROS (Fig. 5) as a potential mediator of necrosis after ciglitazone and apoptosis after troglitazone treatment in Jurkat P^- T cells, we preincubated the cells using different scavengers of ROS for 2 h (Fig. 6). Preincubation with 5 mM NAC (Fig. 6A, column 2) showed no inhibitory effect on ciglitazone-provoked necrosis (set as 100%; Fig. 6A, column 1). In contrast, preincubation of the cells with 300 μM vitamin C could inhibit ciglitazone-mediated necrosis by approximately 40% (Fig. 6A, column 3) and 100 μM MnTBAP, which is a superoxide dismutase mimetic described previously as an effective inhibitor of ROS generation in Jurkat cells (Hildeman et al., 1999; Dolgachev et al., 2003; Huang et al., 2003; Kwon et al., 2003), by approximately 30% (Fig. 6A, column 5). Furthermore, we suggest hydrogen peroxide as another important mediator of ciglitazone-mediated necrosis because preincubation of cells with 100 U catalase inhibited induction of necrosis by approximately 35% (Fig. 6A, column 4). This documented the role of ROS and hydrogen peroxide as likely mediators of ciglitazone-induced necrosis in Jurkat P^- T cells.

Troglitazone-induced apoptosis was not inhibited by 2-h preincubation with 5 mM NAC (Fig. 6B, columns 2) compared with troglitazone-treated cells alone (set as 100%; Fig. 6B, column 1), whereas 300 μM vitamin C and 100 μM MnTBAP reduced apoptosis by approximately 20% each (Fig. 6B, columns 3 and 5). Therefore, ROS production is involved in troglitazone-induced apoptosis in Jurkat P^- cells, although it plays a minor role compared with ciglitazone-induced necrosis. Preincubation of the cells with 100 U catalase showed no significant effect (Fig. 6B, column 4), suggesting that hydrogen peroxide plays no significant role in troglitazone-induced apoptosis.

TZDs Inhibit Complex I of the Mitochondrial Respiratory Chain. Because of the fast depolarization of mitochondrial membrane potential by TZDs (Fig. 2) and the involvement of TZD-evoked ROS (Fig. 5) as a cell death trigger after ciglitazone and troglitazone treatment (Fig. 6), we studied the direct effects of ciglitazone, troglitazone, and rosiglitazone on the mitochondrial respiratory chain using SMPs as a model system. At first, we corroborated TZD effects on NADH-linked respiration (Fig. 7A). Therefore, we initiated respiration in SMPs using NADH as complex I substrate. Basal respiration of untreated controls (0.92 μmol of O

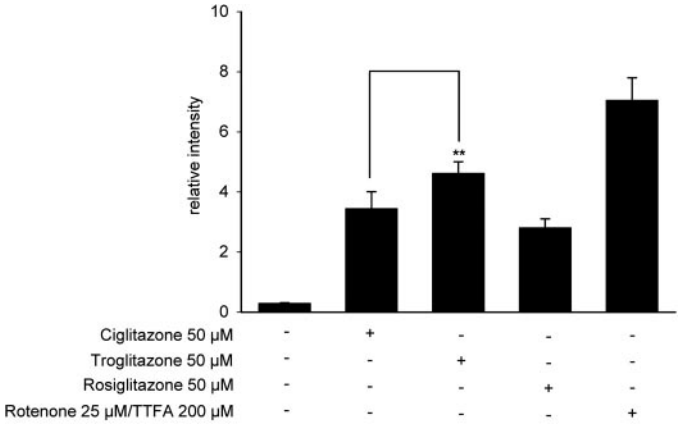

Fig. 5. TZDs provoke the production of ROS in Jurkat P^- cells. H_2DCF-DA-stained cells were incubated with ciglitazone, troglitazone, and rosiglitazone each at 50 μM and the combination of rotenone 25 μM and TTFA 200 μM for 2 h or DMSO as control. ROS were determined using H_2DCF-DA staining as described under *Materials and Methods.* Data are means ± S.E., $n = 6$; **, $P < 0.01$.

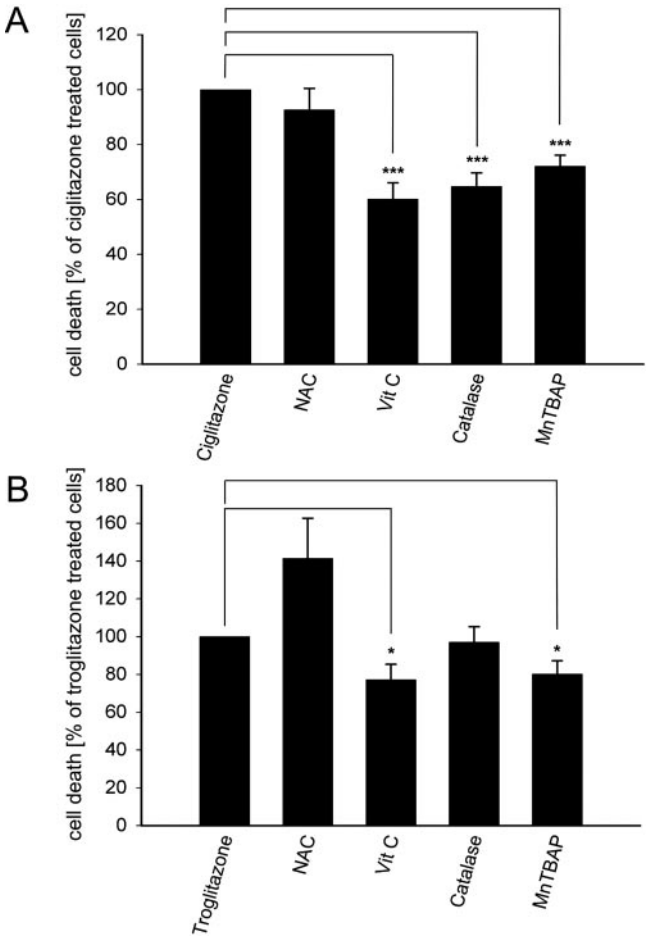

Fig. 6. Ciglitazone-induced necrosis in Jurkat P^- cells is ROS- and hydrogen peroxide-dependent, whereas troglitazone-provoked apoptosis is only partially induced by ROS. Jurkat P^- cells were preincubated for 2 h with 5 mM NAC, 300 μM vitamin C, 100 U of catalase, or 100 μM concentration of the superoxide dismutase mimetic MnTBAP before treatment for 4 h with 50 μM ciglitazone (A) or 50 μM troglitazone (B). Cells were washed and stained with $DiOC_6(3)$. The percentage of $DiOC_6(3)$-negative cells was estimated using flow cytometry as described under *Materials and Methods.* Inhibition of cell death by ROS scavengers is expressed as a percentage of ciglitazone- or troglitazone- induced cell death set as 100%. Data are means ± S.E., $n = 8$; *, $P < 0.05$; ***, $P < 0.001$.

$min^{-1}mg^{-1}$) was set as 100%. We incubated SMPs with increasing concentrations (1–30 μM) of ciglitazone, troglitazone, rosiglitazone (Fig. 7A; ciglitazone, ●; troglitazone, ○; rosiglitazone, ▲), or DMSO as solvent control (data not shown) and analyzed oxygen consumption using an Oxygraph. We identified a concentration-dependent inhibition of respiration with all tested TZDs. Nearly complete inhibition of respiration was detected after incubations with concentrations greater than 10 μM ciglitazone or troglitazone (Fig. 7A), whereas rosiglitazone inhibited respiration by 80% at 30 μM. Because succinate-linked respiration is not affected by rosiglitazone and only affected by higher concentrations of ciglitazone or troglitazone (see below), an effect of TZDs on complex I of the respiratory chain is likely, which is in line with previous studies (Brunmair et al., 2004; Scatena et al., 2004). To verify these findings, we investigated the effect of the three TZDs on the complex I-specific NADH:DBQ activity (Fig. 7B). All three TZDs inhibited the NADH:DBQ activity (basal rate, 0.67 μmol $min^{-1}mg^{-1}$) with the declining potency ciglitazone > troglitazone > rosiglitazone. Compared with the inhibition of the NADH-oxidase, higher concentrations were needed to block NADH:DBQ activity. This difference that was biggest in the case of rosiglitazone could be explained by direct competition with the substrate ubiquinone (DBQ) present in higher concentrations in the complex I activity test and might have been due to the specific properties of the binding domain. It is known that complex I has a relatively large ubiquinone binding pocket containing at least three overlapping binding sites for different classes of inhibitors (Okun et al., 1999a). In the NADH-oxidase measurements, rosiglitazone might have effectively blocked access for the much larger and highly hydrophobic intrinsic substrate Q_{10}, whereas the smaller and more hydrophilic ubiquinone derivative DBQ used in the NADH:DBQ oxidoreductase assay could still enter the quinone reduction site to some extent.

TZDs Differently Affect Complex II of the Mitochondrial Respiratory Chain. We then focused on complex II (Fig. 8) by starting respiration in SMPs using sodium succinate as the complex II substrate. Basal respiration (0.31 μmol O $min^{-1}mg^{-1}$) of untreated controls was set as 100%. We incubated SMPs with increasing concentrations (1–30

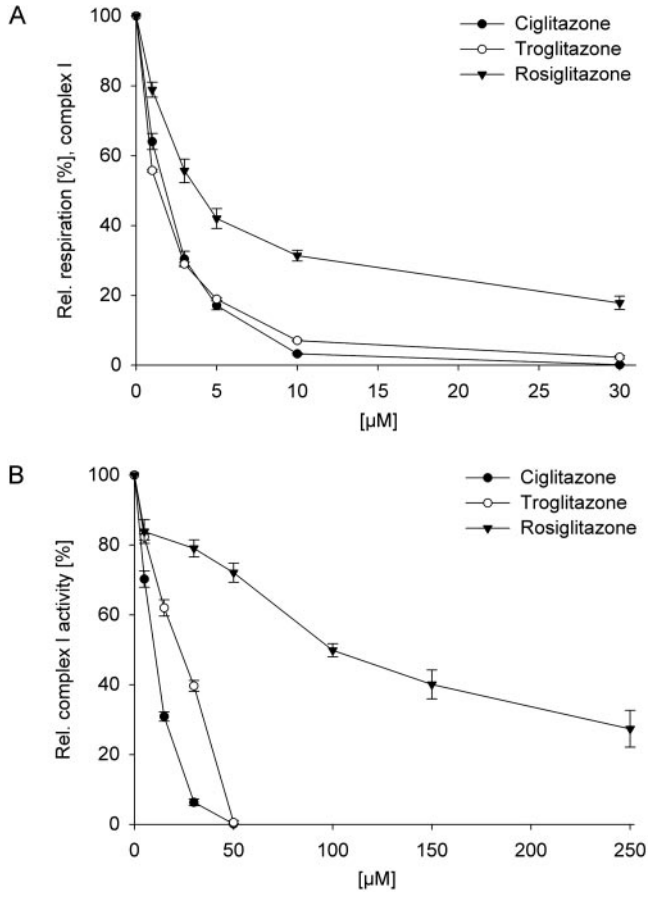

Fig. 7. TZDs inhibit complex I of the mitochondrial respiratory chain. SMPs were prepared as described under *Materials and Methods* and incubated with increasing concentrations (1–250 μM) of ciglitazone, troglitazone, and rosiglitazone. A, respiration in SMPs was initiated by NADH (complex I substrate), and oxygen consumption was detected by an Oxygraph-2K system. Level of respiration was calculated as a percentage of controls. Data are means ± S.D., $n = 3$. B, effect of TZDs on the NADH:DBQ activity of SMPs. The NADH:DBQ activity was determined as described under *Materials and Methods* and related to the uninhibited rate (0.67 μmol $min^{-1}mg^{-1}$) of NADH oxidation. Each point represents the mean value ± S.D. of three independent measurements.

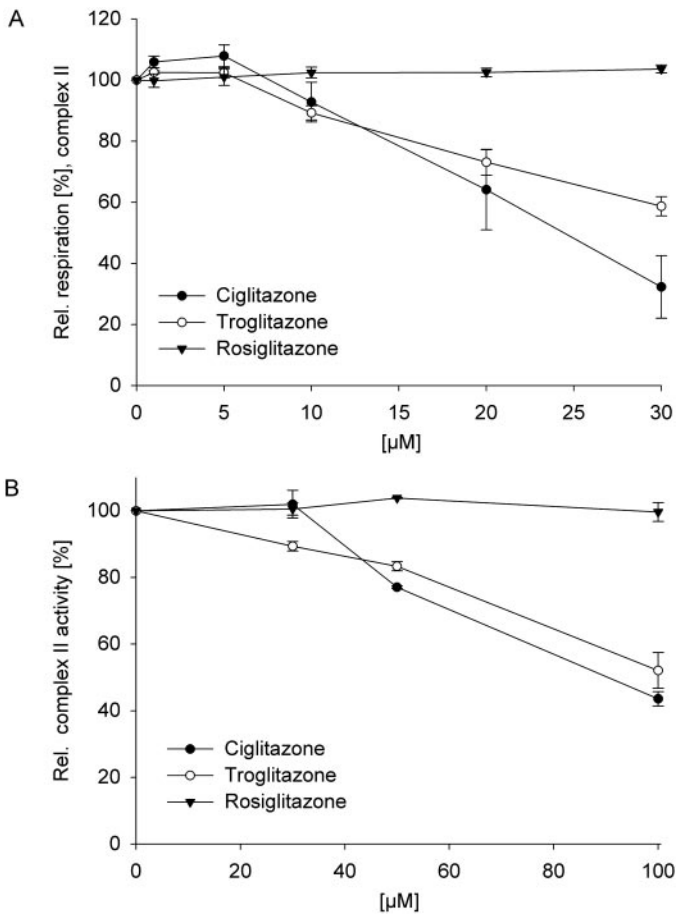

Fig. 8. Ciglitazone and troglitazone inhibit complex II of the mitochondrial respiratory chain. SMPs were prepared as described under *Materials and Methods* and after the addition of the complex II substrate sodium succinate incubated with increasing concentrations (1–100 μM) of ciglitazone, troglitazone, and rosiglitazone. A, respiration in SMPs was detected by measuring oxygen consumption by an Oxygraph-2K system and calculated as percentage of controls. Data are means ± S.D., $n = 3$. B, direct complex II activity was detected as described under *Materials and Methods* after increasing concentrations of TZDs. Data are means ± S.D., $n = 3$.

μM) of ciglitazone, troglitazone, rosiglitazone (Fig. 8A), or DMSO (data not shown) as solvent control and followed oxygen consumption using an Oxygraph. In contrast to rosiglitazone (Fig. 8A), which did not inhibit respiration initiated at complex II, ciglitazone and troglitazone dose-dependently attenuated respiration. Ciglitazone (30 μM) inhibited complex II-initiated respiration by 70%, whereas 30 μM troglitazone reduced it by 40% only (Fig. 8A). In addition, we studied effects of TZDs on the succinate:ubiquinone oxidoreductase activity of complex II in SMPs (Fig. 8B) as described under *Materials and Methods*. The uninhibited rate of DCIP reduction (0.028 μmol $min^{-1}mg^{-1}$) was only approximately 10% of the rate of the succinate oxidase. Higher TZD concentrations were required to inhibit complex II activity compared with relative respiration. However, exposing SMPs to increasing concentrations (30–100 μM) of ciglitazone and troglitazone caused a dose-dependent inhibition of complex II. The maximal effect of nearly 50% inhibition was seen at 100 μM as the highest tested TZD concentration (Fig. 8B). Consistent with results from complex II-initiated respiration (Fig. 8A), rosiglitazone did not alter complex II activity (Fig. 8B). In summary, we identified ciglitazone and troglitazone as complex II inhibitors, whereas rosiglitazone did not affect complex II activity.

Inhibition of Complex II by the Synthetic Inhibitor TTFA Rapidly Induces Apoptosis in Jurkat P⁻ Cells. Based on the results using the SMP model, we investigated the influence of mitochondrial respiration chain inhibition on cell death in Jurkat P⁻ cells. Therefore, we used the established synthetic inhibitors rotenone for complex I and TTFA for complex II of the respiratory chain (Fig. 9). In control experiments, these inhibitors were tested in SMPs to confirm their functionality and specificity as complex I and II inhibitors (data not shown). Using $DiOC_6(3)$ staining, we found that inhibition of complex I by rotenone (Fig. 9A, column 2) only slightly induced cell death (i.e., 10% in Jurkat P⁻ cells), whereas inhibition of complex II by TTFA significantly increased cell death up to 30% (Fig. 9A, column 3) compared with controls (Fig. 9A column 1) or rotenone-treated Jurkat P⁻ cells. Inhibition of complexes I and II by the combination of rotenone/TTFA (Fig. 9A, column 4) increased cell death to 40% compared with controls. To prove apoptosis, cells were treated for 4 h with the combination of rotenone/TTFA and analyzed by DAPI staining. As demonstrated in Fig. 9B (Rot + TTFA), we detected condensed chromatin (highlighted by arrows), pointing at apoptosis as the underlying principle for cell death.

ATP Depletion Switches Apoptotic to Necrotic Cell Death. The ATP level in cells is critical in allowing apoptosis or provoking necrosis. Therefore, we determined the ATP level in Jurkat P⁻ T cells after incubations with ciglitazone, troglitazone, and the combination of rotenone/TTFA (Fig. 10). After a 2-h incubation with 50 or 100 μM ciglitazone (Fig. 10, columns 2 and 3), we found a significant decrease in ATP to approximately 60%, whereas 100 μM troglitazone (Fig. 10, column 4) did not alter the ATP level after 2 h compared with controls (Fig. 10, column 1). Inhibition of complex I and II by the combination of rotenone/TTFA (Fig. 10, column 5) did not change the ATP level compared with controls. As expected, 2-deoxy-D-glucose (2-DG) (Fig. 10, column 6), an established inhibitor of glycolysis, depleted ATP to 40% compared with control cells within a 2-h incubation period.

Combined Inhibition of Complexes I and II along with Depletion of ATP Provokes a Shift from Apoptosis to Necrosis in Jurkat P⁻ T Cells. To study the form of cell death induced by complexes I and II inhibition in combination with ATP depletion, we incubated Jurkat P⁻ cells with the glycolysis inhibitor 2-DG and with the complexes I and II inhibitors rotenone/TTFA (Fig. 11). As shown by annexin V-FITC/PI staining, rotenone/TTFA induced cell death after 4 h with typical characteristics of apoptosis, as represented by mainly annexin V-FITC single-positive cells (Fig. 11; Rot + TTFA, lower right, 18.7%) compared with controls (Fig. 11, control). Depletion of ATP with 2-DG alone, as already shown in Fig. 10, column 6, left cell viability unaltered (Fig. 11, 2-DG versus control). However, 4-h coincubations of cells with 2-DG and the complex I and II inhibitors rotenone/TTFA produced a shift to annexin V-FITC/PI double-positive cells (Fig. 11, 2-DG + Rot + TTFA, upper right, 35.5%), pointing to necrosis as the underlying mode of cell death. Thus, depletion of ATP in Jurkat P⁻ cells in combi-

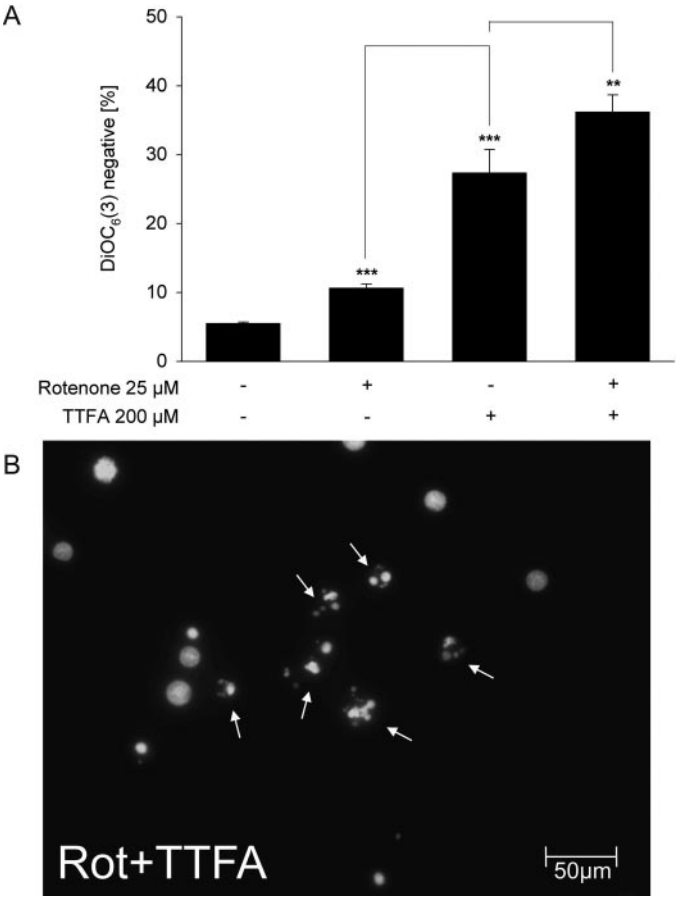

Fig. 9. Inhibition of complex I and II of the respiratory chain provoked apoptosis. Cells were incubated with 25 μM rotenone (inhibitor complex I), 200 μM TTFA (inhibitor complex II), rotenone/TTFA in combination, or remained as controls. A, after incubations for 4 h, cell death was detected by flow cytometry using $DiOC_6(3)$ staining as described under *Materials and Methods*. Cell death is represented as a percentage of $DiOC_6(3)$-negative cells of whole-cell population. Data are means ± S.E., $n = 12$; **, $P < 0.01$; ***, $P < 0.001$. B, representative image of DAPI-stained Jurkat P⁻ cells treated with rotenone and TTFA as described under *Materials and Methods*. Arrows mark condensed chromatin. Magnification, 400×.

nation with inhibition of complex I and II as the apoptotic stimuli provokes a shift from apoptosis to necrosis. These data underscore the importance of decreased ATP levels as an additional factor for ciglitazone-induced necrosis.

Discussion

We focused on PPARγ-independent mechanisms of TZD-induced cell death in Jurkat T cells. Whereas ciglitazone and troglitazone inhibited complexes I and II of the mitochondrial respiratory chain, rosiglitazone affected only complex I. Complexes I and II inhibition by synthetic inhibitors or troglitazone evoked a fast induction of apoptosis. In contrast, ciglitazone induced necrosis. We identified that ciglitazone but not troglitazone additionally causes ATP depletion, thus explaining a shift from apoptosis to necrosis.

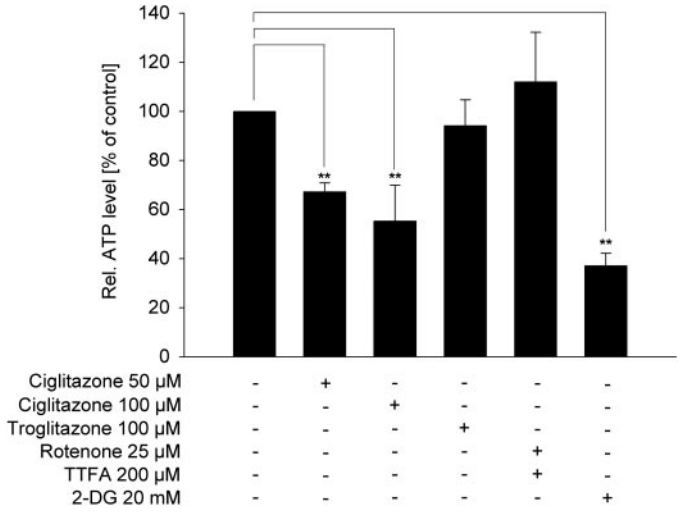

Fig. 10. Ciglitazone decreased the ATP level in Jurkat P$^-$ cells. Jurkat P$^-$ cells were incubated for 2 h with 50 or 100 μM ciglitazone, 100 μM troglitazone, 20 mM 2-DG, the combination of 25 μM rotenone and 200 μM TTFA, or remained as controls. Cells were harvested, and whole-cell ATP was determined as described under *Materials and Methods.* ATP levels are given as a percentage relative to untreated cells (control set as 100%). Values are means ± S.D., $n = 5$; **, $P < 0.01$.

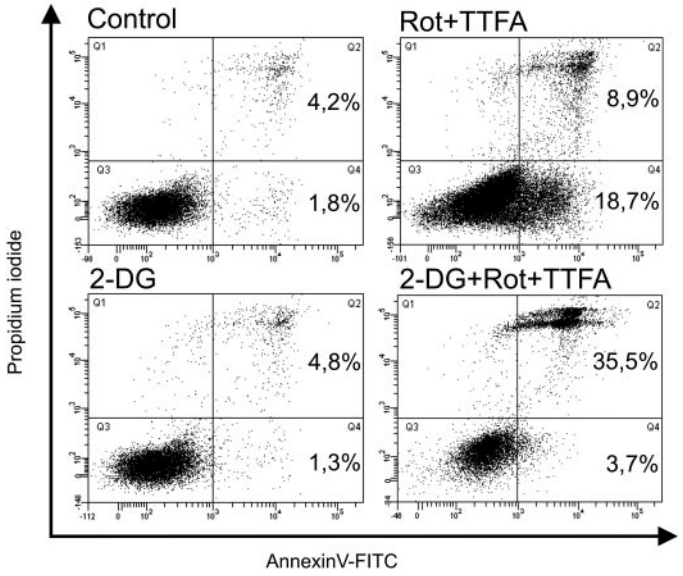

Fig. 11. ATP depletion shifted apoptosis to necrosis. Jurkat P$^-$ cells were incubated with the combination of 25 μM rotenone/200 μM TTFA, 20 mM 2-DG and the combination 2-DG + rotenone/TTFA, or remained as controls. Cells were collected, washed, and stained by annexin V-FITC/PI for flow cytometry as described under *Materials and Methods.* Data are representatives of three separate experiments.

PPARγ activation by TZDs provoked T-cell apoptosis (Harris and Phipps, 2000, 2001, 2002; Tautenhahn et al., 2003; Kanunfre et al., 2004). However, TZDs also activate cell death pathways independent of PPARγ. Considering that TZDs are used as therapeutic agents, understanding PPARγ-dependent and -independent signaling pathways is inevitable. We concentrated on PPARγ-independent effects by using a Jurkat subclone lacking PPARγ mRNA expression under resting conditions and after TZD treatment (Jurkat P$^-$ subclone). Furthermore, TZD concentrations were much higher than their EC_{50} values for PPARγ activation (Willson et al., 1996), therefore disregarding PPARγ-dependent effects.

As reported for HepG2 cells (Tirmenstein et al., 2002; Bova et al., 2005), we found that high troglitazone concentrations provoked apoptotic cell death in Jurkat P$^-$ cells. Ciglitazone elicited fast induction of cell death, which is in line with previous publications (Atarod and Kehrer, 2004; Kanunfre et al., 2004). Rosiglitazone did not alter cell viability at any concentration after 4 h, which is in agreement with data from hepatoma cells (Narayanan et al., 2003).

TZD concentrations used in our study might also mimic therapeutic settings because taking area under the curve (an index of total drug exposure) concentrations into consideration [e.g., area under the curve value for troglitazone reaches 55 μM serum concentration (Feinstein et al., 2005)], a long time exposure to low concentrations can be as effective as shorter exposures to higher concentrations. To prove this, we incubated Jurkat P$^-$ cells with TZDs up to 10 μM for up to 72 h (data not shown). With fetal calf serum being reduced to 2%, at 48 h, necrosis was seen with 10 μM ciglitazone, and apoptosis occurred with 10 μM troglitazone.

Work of others pointed to mitochondria as potential targets in TZD-dependent cell death, showing complex I inhibition for several cell types (Tirmenstein et al., 2002; Dello Russo et al., 2003; Narayanan et al., 2003; Brunmair et al., 2004; et al., 2004; Scatena et al., 2004; Bova et al., 2005). We used SMPs, representing a cell-free test system, to identify the impact of TZDs on the mitochondria respiratory chain. We corroborated previous studies (Brunmair et al., 2004; Scatena et al., 2004) showing that TZDs inhibited complex I, with the discriminating rank order ciglitazone > troglitazone > rosiglitazone. Focusing on complex II of the respiratory chain, we found its inhibition by ciglitazone and troglitazone. This is in contrast to data from Scatena et al. (2004), who mentioned that ciglitazone did not alter succinate dehydrogenase and thus complex II activity in permeabilized HL-60 cells. This can be explained by the different test systems (digitonin-permeabilized cells versus SMPs) and methods used to monitor complex II activity. For a significant determination of succinate dehydrogenase activity, it is necessary to use isolated mitochondria to avoid artificial reduction of electron acceptors by cytosolic enzymes as described by O'Donnell et al. (1995), which is given using SMPs as a test system. Our data proved different TZD concentrations to inhibit complex II as part of the succinate oxidase (which encloses the respiratory chain complexes III and IV) versus the succinate-ubiquinone oxidoreductase activity of complex II. In the latter assay, complex II catalyzes the reduction of respiratory chain component ubiquinone, which subse-

quently reduces DCIP. However, DCIP reduction neither is specific nor does it quantitatively reflect ubiquinone reduction. In some measurements, the known complex II inhibitor TTFA could not reduce a background of approximately 10%. Nevertheless, inhibition of complex II by ciglitazone and troglitazone was detected with both methods, whereas rosiglitazone affected neither succinate oxidase nor the succinate-ubiquinone oxidoreductase activity of complex II.

To corroborate the SMP results with our T-cell model, we investigated effects on cell death in Jurkat P^- cells after respiratory chain inhibition using known complexes I (rotenone) and II (TTFA) inhibitors. Complex I inhibition marginally affected cell death at 4 h. This is in line with studies in HL-60 cells showing significant induction of apoptosis starting 24 h after complex I inhibition by rotenone (Li et al., 2003; Pelicano et al., 2003). Moreover, rosiglitazone, identified as a weaker complex I inhibitor in our study, failed to induce cell death after 4 h. It is interesting that inhibition of complex II by TTFA (Ingledew and Ohnishi, 1977; Zhang and Fariss, 2002) provoked significant cell death after 4 h. The importance of complex II causing rapid effects at the mitochondria was demonstrated previously in human neuroblastoma cells (Fernandez-Gomez et al., 2005), when the complex II inhibitor malonate provoked a fast mitochondrial depolarization. This supports our finding that ciglitazone- and troglitazone-dependent complex II inhibition instantaneously induced cell death. Because ciglitazone and troglitazone also inhibit complex I activity, we analyzed cell death induction after combined inhibition of complexes I and II by rotenone/TTFA. We identified a further increase of cell death compared with inhibition of complex II by TTFA only. This suggests that TZD-dependent inhibition of complexes I and II overlaps to immediately provoke apoptosis. This explains induction of apoptosis after troglitazone treatment but does not rationalize the induction of necrosis by ciglitazone. Previous studies in Jurkat cells by Leist et al. (1997) demonstrated that intracellular ATP levels decide between apoptosis or necrosis after an apoptotic trigger. They suggest that ATP depletion, in combination with an apoptotic stimulus, initiates a switch from apoptosis to necrosis. Recently, a concentration- and time-dependent ATP depletion after ciglitazone treatment was found in explanted Sprague-Dawley rat lenses (Aleo et al., 2005), whereas we observed ATP depletion in Jurkat P^- cells. In line with reports in rat hepatocytes (Haskins et al., 2001), troglitazone and the combination of rotenone/TTFA did not significantly reduce the ATP content. Inhibition of complexes I and II with rotenone/TTFA in combination with ATP depletion by 2-DG switches apoptosis to necrosis, supporting our hypothesis that inhibition of complexes I and II along with ATP depletion by ciglitazone initiated necrosis, whereas troglitazone, leaving the ATP content unaltered, caused apoptosis. However, the mechanisms provoking ciglitazone-mediated ATP depletion remain unclear.

Inhibition of mitochondrial respiration provoked increased ROS production (Pelicano et al., 2003), which we identified as a potential inducer of necrosis after ciglitazone treatment because preincubations with the ROS scavengers vitamin C and MnTBAP showed cytoprotective effects. We also noticed an inhibitory effect of catalase, which is not able to pass the cell membrane, assuming that hydrogen peroxide in the medium plays a contributing role. The efficacy of catalase was confirmed by blocking hydrogen peroxide-induced cell death in Jurkat P^- cells (data not shown). We suggest that ciglitazone provokes ROS production, including hydrogen peroxide, which contributes to necrosis induction in neighboring cells. These data are in contrast to the report of Atarod and Kehrer (2004), showing no protection by vitamin C or catalase, whereas MnTBAP has not been tested in their study. They used higher concentrations of ciglitazone and vitamin C, which might explain the differences. Moreover, necrosis induced by ciglitazone was not completely inhibited by MnTBAP, vitamin C, or catalase. Therefore, we propose that ROS and hydrogen contribute to cell death induction. Vitamin C and MnTBAP also inhibited troglitazone-induced apoptosis, although protection was weaker than observed for ciglitazone-induced necrosis. It is likely that ROS are not the only trigger for troglitazone-induced apoptosis. Because rosiglitazone inhibits complex I of the respiratory chain, we expected production of ROS. However, no significant cell death was observed after 4-h treatment, which may be due to culture conditions (10 versus 2% fetal calf serum) as already mentioned. ROS production not necessarily induces apoptosis as shown by Atarod and Kehrer (2004) when the PPARα agonist WY14643 significantly increases ROS without affecting cell survival even after treatment with 100 μM for up to 48 h. Therefore, we suggest that TZD-evoked ROS contribute to cell death, whereas inhibition of complex II by ciglitazone and troglitazone is the main trigger of cell death. However, the mechanism of cell death induction by inhibition of complex II is still unknown.

Our data suggest that despite their similar structure, TZDs affect cell death by different mechanisms, provoking apoptosis or necrosis. Because TZDs are discussed as potential therapeutic agents for the treatment of cancer and various inflammatory and neurodegenerative diseases (Pershadsingh, 2004), beside their current use for the treatment of diabetes type 2, the mechanisms explored in this study may help in the understanding of possible adverse effects occurring during TZD-based therapies.

Acknowledgments

We thank Ilka Siebels for excellent technical assistance.

References

Aleo MD, Doshna CM, and Navetta KA (2005) Ciglitazone-induced lenticular opacities in rats: in vivo and whole lens explant culture evaluation. *J Pharmacol Exp Ther* **312:**1027–1033.

Atarod EB and Kehrer JP (2004) Dissociation of oxidant production by peroxisome proliferator-activated receptor ligands from cell death in human cell lines. *Free Radic Biol Med* **37:**36–47.

Bova MP, Tam D, McMahon G, and Mattson MN (2005) Troglitazone induces a rapid drop of mitochondrial membrane potential in liver HepG2 cells. *Toxicol Lett* **155:**41–50.

Brunmair B, Staniek K, Gras F, Scharf N, Althaym A, Clara R, Roden M, Gnaiger E, Nohl H, Waldhausl W, et al. (2004) Thiazolidinediones, like metformin, inhibit respiratory complex I: a common mechanism contributing to their antidiabetic actions? *Diabetes* **53:**1052–1059.

Daynes RA and Jones DC (2002) Emerging roles of PPARs in inflammation and immunity. *Nat Rev Immunol* **2:**748–759.

Dello Russo C, Gavrilyuk V, Weinberg G, Almeida A, Bolanos JP, Palmer J, Pelligrino D, Galea E, and Feinstein DL (2003) Peroxisome proliferator-activated receptor gamma thiazolidinedione agonists increase glucose metabolism in astrocytes. *J Biol Chem* **278:**5828–5836.

Dolgachev V, Nagy B, Taffe B, Hanada K, and Separovic D (2003) Reactive oxygen species generation is independent of de novo sphingolipids in apoptotic photosensitized cells. *Exp Cell Res* **288:**425–436.

Feinstein DL, Spagnolo A, Akar C, Weinberg G, Murphy P, Gavrilyuk V, and Russo CD (2005) Receptor-independent actions of PPAR thiazolidinedione agonists: is mitochondrial function the key? *Biochem Pharmacol* **70:**177–188.

Fernandez-Gomez FJ, Galindo MF, Gomez-Lazaro M, Yuste VJ, Comella JX, Aguirre N, and Jordan J (2005) Malonate induces cell death via mitochondrial potential

collapse and delayed swelling through an ROS-dependent pathway. *Br J Pharmacol* **144:**528–537.
Harris SG and Phipps RP (2000) Peroxisome proliferator-activated receptor gamma (PPAR-gamma) activation in naive mouse T cells induces cell death. *Ann NY Acad Sci* **905:**297–300.
Harris SG and Phipps RP (2001) The nuclear receptor PPAR gamma is expressed by mouse T lymphocytes and PPAR gamma agonists induce apoptosis. *Eur J Immunol* **31:**1098–1105.
Harris SG and Phipps RP (2002) Induction of apoptosis in mouse T cells upon peroxisome proliferator-activated receptor gamma (PPAR-gamma) binding. *Adv Exp Med Biol* **507:**421–425.
Haskins JR, Rowse P, Rahbari R, and de la Iglesia FA (2001) Thiazolidinedione toxicity to isolated hepatocytes revealed by coherent multiprobe fluorescence microscopy and correlated with multiparameter flow cytometry of peripheral leukocytes. *Arch Toxicol* **75:**425–438.
Hildeman DA, Mitchell T, Teague TK, Henson P, Day BJ, Kappler J, and Marrack PC (1999) Reactive oxygen species regulate activation-induced T cell apoptosis. *Immunity* **10:**735–744.
Huang HL, Fang LW, Lu SP, Chou CK, Luh TY, and Lai MZ (2003) DNA-damaging reagents induce apoptosis through reactive oxygen species-dependent Fas aggregation. *Oncogene* **22:**8168–8177.
Ingledew WJ and Ohnishi T (1977) The probable site of action of thenolytrifluoracetone on the respiratory chain. *Biochem J* **164:**617–620.
Jaattela M and Tschopp J (2003) Caspase-independent cell death in T lymphocytes. *Nat Immunol* **4:**416–423.
Kanunfre CC, da Silva Freitas JJ, Pompeia C, Goncalves de Almeida DC, Cury-Boaventura MF, Verlengia R, and Curi R (2004) Ciglitazone and 15d PGJ2 induce apoptosis in Jurkat and Raji cells. *Int Immunopharmacol* **4:**1171–1185.
Kersten S, Desvergne B, and Wahli W (2000) Roles of PPARs in health and disease. *Nature (Lond)* **405:**421–424.
Kwon J, Devadas S, and Williams MS (2003) T cell receptor-stimulated generation of hydrogen peroxide inhibits MEK-ERK activation and lck serine phosphorylation. *Free Radic Biol Med* **35:**406–417.
Leist M, Single B, Castoldi AF, Kuhnle S, and Nicotera P (1997) Intracellular adenosine triphosphate (ATP) concentration: a switch in the decision between apoptosis and necrosis. *J Exp Med* **185:**1481–1486.
Leist M, Volbracht C, Fava E, and Nicotera P (1998) 1-Methyl-4-phenylpyridinium induces autocrine excitotoxicity, protease activation, and neuronal apoptosis. *Mol Pharmacol* **54:**789–801.
Li N, Ragheb K, Lawler G, Sturgis J, Rajwa B, Melendez JA, and Robinson JP (2003) Mitochondrial complex I inhibitor rotenone induces apoptosis through enhancing mitochondrial reactive oxygen species production. *J Biol Chem* **278:**8516–8525.
Lowry OH, Rosebrough NJ, Farr AL, and Randall RJ (1951) Protein measurement with the Folin phenol reagent. *J Biol Chem* **193:**265–275.
Narayanan PK, Hart T, Elcock F, Zhang C, Hahn L, McFarland D, Schwartz L, Morgan DG, and Bugelski P (2003) Troglitazone-induced intracellular oxidative stress in rat hepatoma cells: a flow cytometric assessment. *Cytometry A* **52:**28–35.
O'Donnell VB, Spycher S, and Azzi A (1995) Involvement of oxidants and oxidant-generating enzyme(s) in tumour-necrosis-factor-alpha-mediated apoptosis: role for lipoxygenase pathway but not mitochondrial respiratory chain. *Biochem J* **310:**133–141.
Okun JG, Lummen P, and Brandt U (1999a) Three classes of inhibitors share a common binding domain in mitochondrial complex I (NADH:ubiquinone oxidoreductase). *J Biol Chem* **274:**2625–2630.
Okun JG, Zickermann V, and Brandt U (1999b) Properties of the common inhibitor-binding domain in mitochondrial NADH-dehydrogenase (complex I). *Biochem Soc Trans* **27:**596–601.
Pelicano H, Feng L, Zhou Y, Carew JS, Hileman EO, Plunkett W, Keating MJ, and Huang P (2003) Inhibition of mitochondrial respiration: a novel strategy to enhance drug-induced apoptosis in human leukemia cells by a reactive oxygen species-mediated mechanism. *J Biol Chem* **278:**37832–37839.
Pérez-Ortiz JM, Tranque P, Vaquero CF, Domingo B, Molina F, Calvo S, Jordan J, Cena V, and Llopis J (2004) Glitazones differentially regulate primary astrocyte and glioma cell survival. Involvement of reactive oxygen species and peroxisome proliferator-activated receptor-γ. *J Biol Chem* **279:**8976–8985.
Pershadsingh HA (2004) Peroxisome proliferator-activated receptor-gamma: therapeutic target for diseases beyond diabetes: quo vadis? *Expert Opin Investig Drugs* **13:**215–228.
Rybczynski PJ, Zeck RE, Combs DW, Turchi I, Burris TP, Xu JZ, Yang M, and Demarest KT (2003) Benzoxazinones as PPARgamma agonists. Part 1: SAR of three aromatic regions. *Bioorg Med Chem Lett* **13:**2359–2362.
Scatena R, Bottoni P, Martorana GE, Ferrari F, De Sole P, Rossi C, and Giardina B (2004) Mitochondrial respiratory chain dysfunction, a non-receptor-mediated effect of synthetic PPAR-ligands: biochemical and pharmacological implications. *Biochem Biophys Res Commun* **319:**967–973.
Soller M, Tautenhahn A, Brune B, Zacharowski K, John S, Link H, and von Knethen A (2006) Peroxisome proliferator-activated receptor gamma contributes to T lymphocyte apoptosis during sepsis. *J Leukoc Biol* **79:**235–243.
Tautenhahn A, Brune B, and von Knethen A (2003) Activation-induced PPARgamma expression sensitizes primary human T cells toward apoptosis. *J Leukoc Biol* **73:**665–672.
Tirmenstein MA, Hu CX, Gales TL, Maleeff BE, Narayanan PK, Kurali E, Hart TK, Thomas HC, and Schwartz LW (2002) Effects of troglitazone on HepG2 viability and mitochondrial function. *Toxicol Sci* **69:**131–138.
Tolman KG (2000) Thiazolidinedione hepatotoxicity: a class effect? *Int J Clin Pract Suppl* **Oct:**29–34.
Willson TM, Cobb JE, Cowan DJ, Wiethe RW, Correa ID, Prakash SR, Beck KD, Moore LB, Kliewer SA, and Lehmann JM (1996) The structure-activity relationship between peroxisome proliferator-activated receptor gamma agonism and the antihyperglycemic activity of thiazolidinediones. *J Med Chem* **39:**665–668.
Zhang JG and Fariss MW (2002) Thenoyltrifluoroacetone, a potent inhibitor of carboxylesterase activity. *Biochem Pharmacol* **63:**751–754.

Address correspondence to: Dr. Andreas von Knethen, Department of Biochemistry I–Pathobiochemistry, Johann Wolfgang Goethe University, Faculty of Medicine, Theodor-Stern-Kai 7, 60590 Frankfurt/Main, Germany. E-mail: v_knethen@zbc.kgu.de